VOLUME 121, NUMBER 16
APRIL 28, 1999

JOURNAL OF THE AMERICAN CHEMICAL SOCIETY

Far-UV Time-Resolved Circular Dichroism Detection of Electron-Transfer-Triggered Cytochrome *c* Folding

Eefei Chen,[†] Pernilla Wittung-Stafshede,[‡] and David S. Kliger*[,†]

Contribution from the Department of Chemistry & Biochemistry, University of California, Santa Cruz, California 95064, and Chemistry Department, Tulane University, New Orleans, Louisiana 70118

Received September 3, 1998

Abstract: The early dynamics of reduced cytochrome *c* (cyt*c*) folding initiated by a photoinduced electron-transfer reaction are studied using time-resolved circular dichroism spectroscopy. At 3.5 M GdnHCl oxidized cyt*c* is partly unfolded, whereas the reduced form is folded. Thus, under these conditions, rapid electron injection into unfolded, oxidized cyt*c* triggers folding. The kinetics of secondary structure formation in reduced cyt*c* occurs in two major phases. The earliest detection of reduction is accompanied by the appearance of 20% of the secondary structure within 5 μs. From time-resolved absorption and circular dichroism studies this rapid folding is ascribed to a subpopulation of unfolded protein molecules that have a structural tendency to form a native His18-Fe(II)-Met80 ligation. Thereafter, almost no change in the secondary structure is observed until the CD signal starts to decrease in magnitude between 16 μs and 1 ms. This "unfolding" phase ($\tau \approx 180$ μs) is followed by a small increase in the magnitude of the CD signal ($\tau = 6$ ms), forming 30% of the native secondary structure. It appears that a second subpopulation that is initially trapped by a His18-Fe(II)-His26/33 non-native ligation slows down folding until His is displaced by the Met ligand ($\tau = 110$ ms). Formation of 90−95% of the native reduced cyt*c* secondary structure is then detected by ~320 ms.

Introduction

In attempts to identify intermediate species in protein folding mechanisms various approaches for rapidly initiating folding have been coupled with time-resolved optical probes such as absorption,[1−3] infrared,[4,5] circular dichroism (CD),[6,7] fluorescence,[8−12] and resonance Raman[13,14] spectroscopies. Although most of these methods have been used to probe cytochrome *c* (cyt*c*) folding, many of the experimental conditions vary between studies. For example, folding of reduced cyt*c* (redCyt*c*) has been photoinitiated by electron injection into partly unfolded oxidized cyt*c* (oxCyt*c*), whereas folding of oxCyt*c* has been initiated by rapid dilution of the denaturant guanidine hydrochloride (GdnHCl). The results of experiments that use different methods to initiate folding, different forms of cyt*c*, and different concentrations of GdnHCl have provided our current understanding of protein folding in cyt*c*.

For studies of redCyt*c* with nanosecond to microsecond time

* Author to whom correspondence should be sent.
[†] University of California.
[‡] Tulane University.

(1) Wittung-Stafshede, P.; Gray, H. B.; Winkler, J. R. *J. Am. Chem. Soc.* **1997**, *119*, 9562−9563.
(2) Pascher, T.; Chesick, J. P.; Winkler, J. R.; Gray, H. B. *Science* **1996**, *271*, 1558−1560.
(3) Jones, C. M.; Henry, E. R.; Hu, Y.; Chan, C.-K.; Luck, S. D.; Bhuyan, A.; Roder, H.; Hofrichter, J.; Eaton, W. A. *Proc. Natl. Acad. Sci. U.S.A.* **1993**, *90*, 11860−11864.
(4) Gilmanshin, R.; Williams, S.; Callender, R. H.; Woodruff, W. H.; Dyer, R. B. *Proc. Natl. Acad. Sci. U.S.A.* **1997**, *94*, 3709−3713.
(5) Williams, S.; Causgrove, T. P.; Gilmanshin, R.; Fang, K. S.; Callender, R. H.; Woodruff, W. H.; Dyer, R. B. *Biochemistry* **1996**, *35*, 691−697.
(6) Chen, E.; Wood, M. J.; Fink, A. L.; Kliger, D. S. *Biochemistry* **1998**, *37*, 5589−5598.

10.1021/ja983169+ CCC: $18.00
Published on Web 04/13/1999

resolution, two methods have been used to initiate folding, ligand dissociation of the partly unfolded CO bound reduced form (COCyt*c*),[3,6] and electron injection into partly unfolded oxCyt*c*.[2,15] Each method relies on the differences in the folding free energies for oxCyt*c* or COCyt*c* and redCyt*c*, as well as the linear dependence of their folding free energies on the concentration of GdnHCl. These factors are apparent in the titration of redCyt*c* and oxCyt*c* with GdnHCl, where the fraction of unfolded protein in oxCyt*c* and folded protein in redCyt*c* are near 1 in the range of 3−4 M GdnHCl.[2] A similar difference in the folding curves for redCyt*c* and COCyt*c*[3,16] indicates that COCyt*c* is more stable toward unfolding than redCyt*c*. Thus, injection of an electron into unfolded oxCyt*c* or photolysis of unfolded COCyt*c* is expected to rapidly generate the initially unfolded form of redCyt*c*, which subsequently folds into its equilibrium native conformation.

The earliest events detected in time-resolved absorption (TROD) studies of redCyt*c* folding initiated by ligand photodissociation, 2 and 50 μs, have been assigned to the formation of His18-Fe(II)-Met80 and His18-Fe(II)-His26/33 (bis-His) ligations, respectively.[3,6,7,17] At longer times CO rebinding competes with folding and favors the unfolded conformation of the ligated protein. Even at the earliest CO rebinding event ($\tau = 225$ μs) the percentage of folded protein detected by far-UV time-resolved circular dichroism (TRCD) methods is small. In these studies a 2-μs His18-Fe(II)-Met ligation step is accompanied by formation of only 8% of the native secondary structure that is observed in the CO unbound redCyt*c* structure.[6] Further secondary structure formation is not observed for two major reasons: protein folding in the presence of 4.6 M GdnHCl (pH 6.5) is much slower than CO rebinding, which favors the partly unfolded state, and a 50-μs bis-His intermediate inhibits the folding process. Previous studies have assigned misfolded transients by changing sample conditions and observing the effects on the rate of folding. For example, using time-resolved resonance Raman (TR^3) spectroscopy to probe the structural changes in oxCyt*c* folding that follow rapid dilution of GdnHCl, a similar misligated bis-His transient as that suggested in the reaction of photolyzed COCyt*c*[6] was suggested to form within the 100-μs dead time of the mixing apparatus. By decreasing the pH of the oxCyt*c* folding experiment below 5, which results in protonation of His26/33, the resonance Raman data showed an increase in the time constant of the process that was correlated with protein folding.[13,14]

The above studies raise the question of whether intermediates involving non-native ligations impede or play another important role in protein folding. Is such an intermediate necessary to guide the folding process because the protein has folded improperly or is the off-pathway intermediate a dead-end result of a misfolding step? The results of TR^3 studies suggest that oxCyt*c* folds through an obligatory His18-Fe(III)-water intermediate and that, depending on the pH of the denatured state, two off-pathway (or misligated) intermediates, a bis-His and a 5-coordinate high-spin species, convert back to the His18-Fe(III)-water species during the random fluctuations that guide the search for the native protein conformation.[14,18] Formation of the bis-His mis-coordinated species is suggested to be accompanied by misfolding of a polypeptide segment, which is then expected to unravel before it can proceed to the native state. Other time-resolved spectroscopies, such as far-UV CD, would be useful to confirm this redirection of folding.

To date the fastest observation of secondary structure changes in cyt*c* have been reported by stopped-flow CD experiments.[19,20] With a dead time of 4 ms, which is about 4.5 times faster than that in the studies by Kuwajima and co-workers,[19] Elöve et al.[20] showed that 44% of the native oxCyt*c* CD signal at 222 nm appears within the time resolution of the instrument. A kinetic study of this "burst phase" can provide information on how many intermediates participate in the fast formation of secondary structure, on what time scale the secondary structure appears, and perhaps on how a misligated species, such as the 50 μs bis-His component observed in TROD studies of redCyt*c*,[6] influences protein folding. Using time-resolved CD (TRCD) spectroscopy, coupled with photoinduced electron transfer from NADH to trigger folding,[1,21,22] we have probed the early dynamics of protein folding in redCyt*c*. The results of these far-UV TRCD studies indicate that in less than 4 ms there is formation of ~25% of the native structure. The kinetics of secondary structure formation can be described by an early 5-μs intermediate, at which time ~20% of the native structure is observed, a small "unfolding" feature ($\tau \approx 180$ μs) between 16 μs and 1 ms, and two slower intermediates with time constants of 6 and 110 ms. The importance of studying the "burst phase" is underscored by the suggestion that this phase is not characterized by the formation of intermediates with high levels of secondary structure but rather by the initial response of the unfolded protein to the solvent changes induced by rapid dilution of denaturant.[23,24] The intermediates observed here are clearly not of this nature since folding was initiated without changing the solvent conditions.

Materials and Methods

Sample Preparation. Horse heart cyt*c* and NADH were purchased from Sigma Chemical Co., sodium hydrosulfite (dithionite) from Fluka, ultrapure GdnHCl was obtained from ICN Biomedicals, Inc., and sodium phosphate (NaP, monobasic, Na_2HPO_4, and dibasic, NaH_2PO_4) from Fisher Scientific. All chemicals were used without further purification.

Cyt*c* samples for TRCD experiments were prepared by adding separately deoxygenated solid cyt*c* (~100 μM) and NADH (450−550 μM) to Ar-saturated buffer solutions (0.1 M NaP, 3.5 M GdnHCl, pH 7), which were then transferred to an Ar-saturated glovebag. A peristaltic pump, kept in the glovebag, was used to control recycled

(7) Goldbeck, R. A.; Thomas, Y. G.; Chen, E.; Esquerra, R. M.; Kliger, D. S. *Proc. Natl. Acad. Sci. U.S.A.* **1998**, *96*, 2782−2787.
(8) Chan, C.-K.; Hofrichter, J.; Eaton, W. A. *Science* **1996**, *274*, 628−629.
(9) Chan, C.-K.; Hu, Y.; Takahashi, S.; Rousseau, D. L.; Eaton, W. A.; Hofrichter, J. *Proc. Natl. Acad. Sci. U.S.A.* **1997**, 1779−1784.
(10) Nölting, B.; Golbik, R.; Fersht, A. R. *Proc. Natl. Acad. Sci. U.S.A.* **1995**, *92*, 10667−10672.
(11) Ballew, R. M.; Sabelko, J.; Gruebele, M. *Proc. Natl. Acad. Sci. U.S.A.* **1996**, *93*, 5759−5764.
(12) Ballew, R. M.; Sabelko, J.; Gruebele, M. *Nat. Struct. Biol.* **1996**, *3*, 923−926.
(13) Takahashi, S.; Yeh, S.-R.; Das, T. K.; Chan, C.-K.; Gottfried, D. S.; Rousseau, D. L. *Nat. Struct. Biol.* **1997**, *4*, 44−50.
(14) Yeh, S.-R.; Takahashi, S.; Fan, B.; Rousseau, D. L. *Nat. Struct. Biol.* **1997**, *4*, 51−56.
(15) Mines, G. A.; Pascher, T.; Lee, S. C.; Winkler, J. R.; Gray, H. B. *Chem. Biol.* **1996**, *3*, 491−497.
(16) Wood, M. J. Unpublished results.
(17) Hagen, S. J.; Hofrichter, J.; Szabo, A.; Eaton, W. A. *Proc. Natl. Acad. Sci. U.S.A.* **1996**, *93*, 11615−11617.
(18) Yeh, S.-R.; Rousseau, D. L. *Nat. Struct. Biol.* **1998**, *5*, 222−228.
(19) Kuwajima, K.; Yamaya, H.; Miwa, S.; Sugai, S.; Nagamura, T. *FEBS Lett.* **1987**, *221*, 115−118.
(20) Elöve, G. A.; Chaffotte, A. F.; Roder, H.; Goldberg, M. E. *Biochemistry* **1992**, *31*, 6876−6883.
(21) Wittung-Stafshede, P.; Malmström, B. G.; Winkler, J. R.; Gray, H. B. *J. Phys. Chem.* **1998**, *102*, 5599−5601.
(22) Telford, J. R.; Wittung-Stafshede, P.; Gray, H. B.; Winkler, J. R. *Acc. Chem. Res.* **1998**, *31*, 755−763.
(23) Fersht, A. R. *Proc. Natl. Acad. Sci. U.S.A.* **1995**, *92*, 10869−10873.
(24) Sosnick, T. R.; Mayne, L.; Englander, S. W. *Proteins: Struct. Funct. Genet.* **1996**, *24*, 413−426.

flow from a sample reservoir to a 0.5-mm path length sample cell with fused silica windows.

For equilibrium CD measurements cyt*c* samples were prepared both with and without NADH in the 0.1 M NaP−3.5 M GdnHCl buffer solutions. The redCyt*c* for steady-state measurements was prepared by adding sodium dithionite to oxCyt*c*. The steady-state CD spectra were collected using a 0.5-mm path length fused silica circular cell.

Steady-State Circular Dichroism Experiments. Equilibrium CD spectra were measured on an AVIV 62 DS CD spectrometer (AVIV Associates, Lakewood, NJ). CD data were integrated over 5 s every 1 nm using a 0.5-nm bandwidth in the 200−300-nm spectral range. The temperature of the sample was stabilized at 23−25 °C during data accumulation.

Photoinduced Electron-Transfer Experiments. The transfer of an electron from NADH to cyt*c* follows absorption of a photon from a Quanta Ray DCR-11 Nd:YAG frequency upconverted laser. The ∼7 ns (full width at half-maximum), 355 nm, ∼36 mJ pulse has a 6 mm × 5 mm cross section. Spectral changes resulting from the electron transfer event were probed with a xenon flash lamp. The laser and probe beams entered the cell at an angle of 30°, with the probe beam propagation axis normal to the face of the sample. The probe beam was focused onto the slit of a spectrograph and detected by a gated optical multichannel analyzer (OMA). The details of the TROD and TRCD system have been described previously[25,26] and will not be discussed here.

Data were collected with a 2-s delay between each laser flash. The sample was flowed continuously at a rate of ∼8 μL/s for data collection at time delays between 1 μs and 50 ms. This flow rate was fast enough to move the irradiated volume of 11.8 μL out of the pump−probe path before the subsequent laser pulse. For time delays greater than 50 ms the sample was flowed only between laser pulses. These precautions help to ensure that the TRCD and TROD difference spectra were not masked by the build-up of photoinjection and/or photodegradation products and that the reduced sample did not flow out before detection. The temperature was stabilized at 23−25 °C throughout the experiment by using a cooling bath coupled to a heat/cooling jacket that is attached to the flow cell or by maintaining a steady flow of nitrogen across both window faces of the flow cell. In either case the temperature was checked periodically throughout the experiment at the flow cell by using an infrared temperature probe (Fluke 80T-IR, Fluke Corporation, Everett, WA).

Two sets of TROD data were measured before almost every set of TRCD data. The TROD data were measured at 30 time delays after photoinitiation of the protein folding reaction (2 averages each). The results of the TROD studies will not be discussed here, with the exception of aspects which are important to understanding the TRCD data, but will be presented in a future publication. The TRCD data comprise 512−1024 averages for each of the 32 time delays, from 2 μs to 1 s, after photoinjection. A steady-state UV/vis spectrum (Shimadzu UV-2101PC spectrophotometer and TROD apparatus) of oxCyt*c* was measured at the beginning of the experiments and equilibrium CD and UV/vis spectra of redCyt*c* were measured on the TRCD and TROD apparati at the end of all experiments.

Because the sample was recycled between the sample reservoir and the flow cell, it was important to check the sample frequently for signs of redCyt*c* build-up. For TROD data collection, a spectrum obtained 1-ms after photolysis was measured at the beginning of the experiments and compared to 1 ms spectra collected randomly throughout the experiment. The build-up of photoreduction product is evident by a decrease in intensity of the TROD spectrum obtained 1 ms after photoinjection. For TRCD experiments, the initial state CD spectrum of oxCyt*c* was measured between every 2−3 time-resolved scans. Once the level of redCyt*c* in the sample was detectable in the initial state CD or 1 ms TROD spectra the sample was exposed to oxygen in order to reform oxCyt*c* and then deoxygenated for ca. 15 min. It was a requirement that the UV/vis spectrum of the regenerated sample overlay the spectrum of fresh oxCyt*c* (in the region of 280−650 nm) before TRCD measurements could continue. If necessary, NADH was added to maintain its initial concentration.

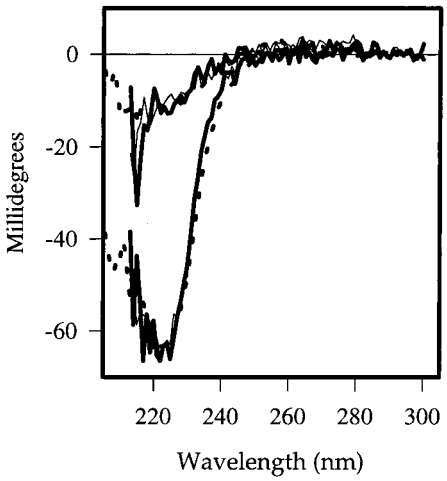

Figure 1. Equilibrium CD spectra of oxCytc and redCytc. These spectra were measured under different conditions at pH 7: 0.1 M NaP−3.5 M GdnHCl with (thin black) and without (thick black) 500 μM NADH on a conventional CD instrument and with NADH on the TRCD apparatus (dotted black). This comparison demonstrates that in 3.5 M GdnHCl redCyt*c* is more stable toward folding than oxCyt*c*, that NADH does not influence the equilibrium secondary structure of cyt*c*, and that the TRCD apparatus reports CD data comparable to that obtained on the conventional CD instrument. All spectra were obtained using a 0.5-mm path length cell and a sample concentration of ∼100 μM. The spectra measured on the CD spectrometer were collected with a 5-s integration time every 1 nm over the 200−300-nm spectral range using a 0.5-nm bandwidth. Each CD spectrum obtained from the TRCD instrument represents an average of ∼2000 scans. The characteristic peptide band is cut off below 215 nm because GdnHCl and NADH absorb much of the far-UV light in this region.

Data Analysis. TRCD data are presented as multiwavelength spectra from 210 to 270 nm and as a kinetic signal obtained by averaging the OMA TRCD data at different times over the 220−225-nm spectral range. The multiwavelength data were analyzed using singular value decomposition (SVD) and global analysis procedures. Algorithms for these methods were written with the mathematical software package Matlab (Pro-Matlab, The Math Works, Inc., South Natick, MA). SVD and global analyses will not be discussed here. However, readers are directed to previously published details of SVD and global analyses that are discussed with respect to heme proteins,[27,28] to COCyt*c*,[6] and to far-UV TRCD studies.[26]

Results

Figure 1 shows the equilibrium CD spectra of oxCyt*c* and redCyt*c* obtained under various conditions: 0.1 M NaP−3.5 M GdnHCl (pH 7) with and without 500 μM NADH on a conventional CD instrument and with NADH on the TRCD apparatus. The CD signal at 222 nm for oxCyt*c* is approximately 6 times less intense than that for redCyt*c* in 3.5 M GdnHCl. The folding curves indicate that the fraction of folded protein in redCyt*c* and of unfolded protein in oxCyt*c* are near 1 when titrated against 3−4 M GdnHCl.[2] The spectra of samples with ∼500 μM NADH overlay the spectra of samples without NADH. Thus there are no detectable influences of NADH on the equilibrium secondary structure for both oxCyt*c* and redCyt*c*. The equilibrium spectra of oxCyt*c* and redCyt*c* (0.1 M NaP−3.5 M GdnHCl−500 μM NADH, pH 7) measured on the TRCD apparatus are also compared to those obtained on the AVIV

(25) Zhang, C. F.; Lewis, J. W.; Cerpa, R.; Kuntz, I. D.; Kliger, D. S. *J. Phys. Chem.* **1993**, *97*, 5499−5505.

(26) Chen, E.; Lapko V. N.; Song, P.-S.; Kliger, D. S. *Biochemistry* **1996**, *36*, 4903−4908.

(27) Henry, E. R.; Hofrichter, J. *Methods Enzymol.* **1992**, *210*, 129−192.

(28) Goldbeck, R. A.; Kliger, D. S. *Methods Enzymol.* **1993**, *226*, 147−177.

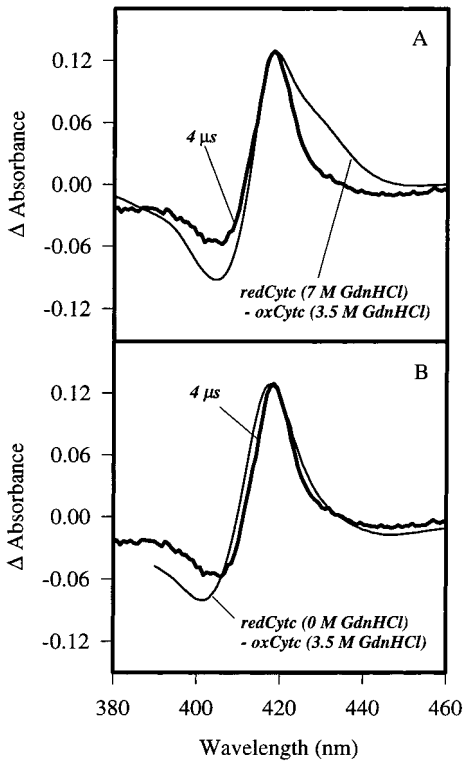

Figure 2. Comparison of the 4-μs TROD difference absorption spectrum (thick line) with equilibrium difference spectra of redCytc minus oxCytc. The difference between redCyt*c* (7 M GdnHCl) and oxCyt*c* (3.5 M GdnHCl) (A, thin line) should reflect largely changes at the heme iron upon formation of the bis-His reduced species. In contrast the difference spectra of folded redCyt*c* (0 M GdnHCl) and partially unfolded oxCyt*c* (3.5 M GdnHCl) should reflect changes upon forming reduced species with the native Met ligation (B, thin line). These two comparisons suggest that the earliest detection of photoreduction product is accompanied by formation of the His18-Fe(II)-Met ligation rather than the bis-His ligation. The equilibrium spectra were measured with a 1 mm quartz cuvette on a UV/vis spectrophotometer, while the TROD spectrum was obtained with a 0.5 mm path length flow cell. The equilibrium spectra were normalized to match the intensity of the TROD absorbance maximum.

CD spectrometer. This comparison indicates that the TRCD apparatus accurately reports the CD spectra of cyt*c*. The oxCyt*c* and redCyt*c* spectra obtained from the TRCD apparatus represent an average of ~2000 scans. Because GdnHCl and NADH absorb much of the far-UV light, the spectra are reliable only at wavelengths greater than 210 nm.

Upon excitation of NADH, reactive species are generated that rapidly reduce unfolded oxCyt*c*.[22] Because the change in heme oxidation state will be a significant component of the Soret absorption band, it is difficult to sort out contributions due to protein folding versus heme reduction with the TROD technique. However, since the spectrum in the Soret region is more sensitive to the heme oxidation and ligation states, it can be used to determine when reduction occurs after excitation. In Figure 2 a TROD difference absorption spectrum measured 4 μs after photoinitiation of folding is compared to the equilibrium difference spectra of redCyt*c* in 7 M GdnHCl and oxCyt*c* in 3.5 M GdnHCl (Figure 2a) and of native redCyt*c* (0 M GdnHCl) and oxCyt*c* in 3.5 M GdnHCl (Figure 2b). In 7 M GdnHCl redCyt*c* comprises greater than 95% His18-Fe(II)-His ligations.[29] This is in contrast to the His18-Fe(II)-Met ligand found in the

(29) Thomas, Y. G.; Goldbeck, R. A.; Kliger, D. S. Manuscript in preparation.

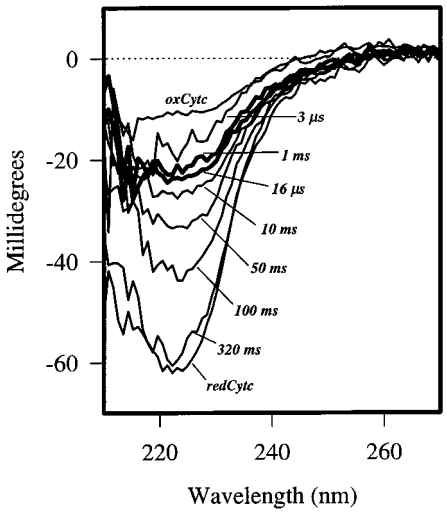

Figure 3. Far-UV TRCD results of redCytc folding induced by photoinjection. Although TRCD spectra were measured at 32 time points after the initial photoevent, only 7 time points are shown above: 3 and 16 μs, 1, 10, 50, 100, and 320 ms. The spectra measured at 16 μs and 1 ms are shown in thicker black to highlight the dynamics of the CD signal in that time region. Each spectrum represents the average of at least 512 scans. SVD and global analysis of the TRCD data reports three exponential processes with lifetimes (and amplitudes) of 5 $\pm$ 1.4 μs (0.33), 6 $\pm$ 2 ms (0.06), and 110 $\pm$ 8 ms (0.24). The data were accumulated with 100 μM cyt*c* in 0.1 M NaP−3.5 M GdnHCl−500 μM NADH, pH 7 using a 0.5-mm path length flow cell.

native reduced protein. In the comparison provided by Figure 2, the 4-μs TROD spectrum more closely resembles the equilibrium difference spectrum of native redCyt*c* and partially unfolded oxCyt*c* (3.5 M GdnHCl). Thus, reduction and formation of a His18-Fe(II)-Met ligation in some protein molecules appears to occur within 4 μs after NADH excitation.

TRCD data were measured at 32 time points after the initial photoevent. For clarity of presentation, Figure 3 shows the data for only 7 time delays: 3 and 16 μs, 1, 10, 50 100, and 320 ms. The spectra measured at 16 μs and 1 ms are highlighted (heavy black lines) to show the dynamics of the CD signal (millidegrees) in that time region. A plot of the difference CD of the photoreduction product minus oxCyt*c* (Δmillidegrees) versus the logarithm of time, Figure 4a, is presented to describe more graphically the kinetic behavior of the TRCD signals in the 220−225-nm spectral region. An initial increase of the negative CD signal until ~16 μs is followed by a slight decrease in the signal magnitude between 16 μs and 1 ms. After 1 ms the magnitude of the negative CD signal increases monotonically. At ~320 ms the magnitude of the CD signal is 90−95% of the native CD signal. Beyond 800 ms the magnitude of the signal begins to decrease (data not shown). This decay is probably due to oxidation of redCyt*c* by trace levels of oxygen, which explains in part the formation of only 90−95% redCyt*c*. In addition, MCD data show that up to ca. 5% redCyt*c* is present in the initial solution of oxCyt*c*.[29] Because this percentage of redCyt*c* is not affected by the electron-transfer step it does not contribute to the difference spectra used in the data analysis.

The TRCD data, including all 32 time delays, were analyzed as the difference of the photoreduction product spectra and the initial state spectrum of oxCyt*c*. SVD and global analysis of the TRCD data reliably generated three exponential processes with lifetimes of 5 μs, 6 ms, and 110 ms. A fourth exponential could be fit to the data, but was unstable, yielding a lifetime of either 40 or 215 μs for different experiments. However, the single wavelength data shown in Figure 4 could be fit to four

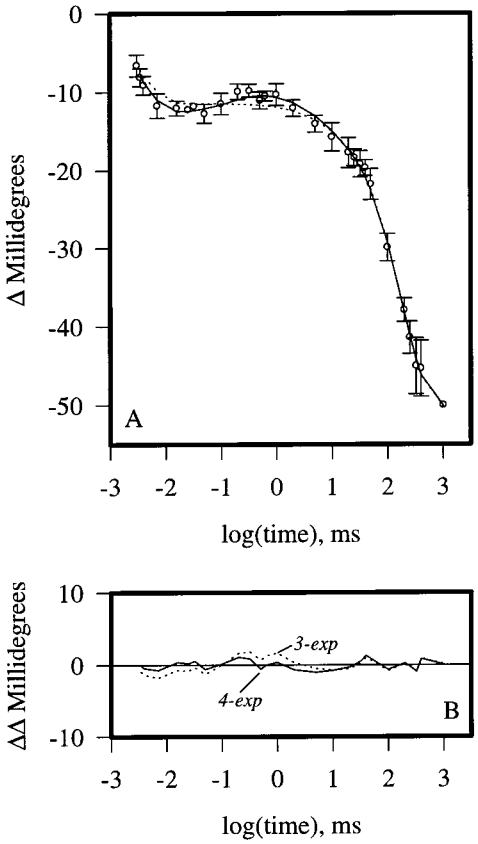

Figure 4. Time dependence of the TRCD signals averaged between 220 and 225 nm. This plot shows all 32 times points that are discussed in Figure 3, giving more kinetic detail of the behavior of the TRCD signal (A). The difference TRCD data of the photoreduction product minus the initial state oxCytc are averaged between 220 and 225 nm. The time region highlighted in Figure 3 is characterized by a minimum near 16 μs and a maximum near 1 ms. Attempts to fit a fourth exponential value to the data in Figure 3 (using SVD and global analysis) generates either 40 or 215 μs. However, a fourth exponential process with a lifetime of 180 μs could be fit to the single wavelength profile of the TRCD data (solid). A comparison of the four-exponential decay with a three-exponential fit (3.5 μs, 6 ms, and 180 ms, dashed) in A and of the residuals for the two fits (4-exp, solid; 3-exp, dashed) in B show that the data is better described with the inclusion of the 180-μs component.

exponential processes with lifetimes of ca. 3.5 and 180 μs and 6 and 180 ms. The comparisons of the four-exponential fit to a three component fit of 3.5 μs, 6 ms, and 180 ms (Figure 4a) and of the residuals of the two fits (Figure 4b) show that the data is better described when a 180-μs process is included. The instability of the four-component fit in the global analysis of the multiwavelength data is probably due to the small changes in CD signal, relative to the noise, between 16 μs and 1 ms. The significance of the 180-μs "unfolding" process in this time region is under further investigation.

Discussion

The burst phase (<4 ms) reported in the stopped-flow study of secondary structure dynamics in cyt*c* folding[20] is kinetically resolved in the present study, allowing observation of the early onset of secondary structure. By using fast photoinitiation methods with structure-sensitive probes of protein structure, such as CD, it is possible to monitor folding events during this burst phase. Taking advantage of the differences in the folding free energies of oxCyt*c* and redCyt*c* and of the linear dependence of these free energies on the concentration of GdnHCl, we have chosen to study the folding of redCyt*c* induced by photoinjection of an electron from the reducing agent NADH into partially unfolded oxCyt*c* (3.5 M GdnHCl) using TRCD spectroscopy.

The mechanism by which NADH reduces oxCyt*c* is a two-photon reaction that generates two strong reducing agents, a hydrated e^-_{aq} and an NAD$^\bullet$ radical, upon high-intensity irradiation with 355-nm light.[30] According to studies of native oxCyt*c* reduction by photoexcited NADH,[31] the first electron-transfer event is estimated to have a first-order rate constant of 4.6×10^6 s^{-1}, giving a time constant of ~200 ns. At this time an NAD$^\bullet$ radical is also generated by deprotonation of $^\bullet$NADH$^+$. Because only ~34% of the NAD$^\bullet$ radicals reduce oxCyt*c* ($k = 2 \times 10^9$ M^{-1} s^{-1}),[31] redCyt*c* is expected from this reduction within 15 μs. In the presence of GdnHCl these reduction processes may occur faster because the heme group, surrounded by a partially unraveled protein environment, is more accessible to NADH.

With NADH as the source of electrons it is thus possible to use photoinjection methods to follow the dynamics of secondary structure formation in redCyt*c* from as early as a few microseconds to as late as seconds following photoreduction. The changes in the CD signal that follow photoinitiation are attributed to formation of secondary structure rather than to heme or aromatic residue interactions or to the spectral dynamics of the NADH photoproducts. This assignment is based predominantly on the spectral shapes of the TRCD signals. To determine whether NADH photoproducts can contribute to the TRCD signals, several control conditions were examined. First, photoinjection into folded oxCyt*c* in the presence of 0.1 M NaP (0 M GdnHCl) and 500 μM NADH resulted only in the formation of a CD spectrum that resembled the equilibrium CD spectrum for redCyt*c*. Second, TRCD measurements at 1.5 and 2 μs showed a positive feature near 210 nm that is characteristic of the equilibrium CD spectrum of the NADH photoproduct. By 3 μs the positive CD band is no longer present.

Although the heme−protein coupling increases as the protein folds, its contribution to the far-UV CD is not considered to be significant. Rather, CD and optical rotatory dispersion studies of heme insertion into apomyoglobin suggest that heme transitions centered 50−100 nm away from the n−π* peptide transition would more likely contribute to the optical rotation at 233 nm.[32] In contrast, aromatic residues can influence the far-UV CD signals with positive bands in the 215−230 nm region, particularly if the content of helix is low.[33] This influence would be most evident at the start of protein folding, where the helix content is just beginning to increase from the initially unfolded redCyt*c*. The TRCD signals in Figure 3 should then reflect the convolution of positive bands around 215−230 nm. However, these spectral profiles, although limited to wavelengths greater than 210 nm, are consistent with the equilibrium CD spectra characteristic of secondary structure in native cyt*c*.

The time dependent behavior of the CD signal in the far-UV region is described reliably by three components with lifetimes of 5 μs, 6 ms, and 110 ms. A fourth component of 180 μs could only be fit reliably to the single wavelength profile of the TRCD data (Figure 4). In this paper the 5-μs, 180-μs, and 6-ms processes will be identified with the burst phase of folding, whereas the 110 ms component will be associated with a slow

(30) Czochralska, B.; Lindqvist, L. *Chem. Phys. Lett.* **1983**, *101*, 297−299.
(31) Orii, Y. *Biochemistry* **1993**, *32*, 11910−11914.
(32) Breslow, E.; Beychok, S.; Hardman, K. D.; Gurd, G. R. N. *J. Biol. Chem.* **1965**, *240*, 304−309.
(33) Woody, R. W. *Circular Dichroism: Principles and Applications*; VCH Publishers: New York, 1994; pp 473−496.

phase of folding (which was identified in stopped flow CD studies[20] as the fast folding phase). The 5-μs process is a global snapshot of the rapid formation of 20% secondary structure that is facilitated by the reduction of partly unfolded oxCyt*c*. This assignment is supported by comparison of the TROD spectra collected at 4 μs with equilibrium difference spectra measured under different concentrations of GdnHCl. While this comparison suggests that both reduction and folding processes are detectable within 4 μs, the results of time-resolved magnetic circular dichroism (TRMCD) studies[34] provide direct evidence for the early formation of a His18-Fe(II)-Met ligation, $\tau = 1.5$ μs. The 5-μs time constant is slower than the 50−500-ns lifetime reported for the more localized secondary structure formation in time-resolved infrared studies of apomyoglobin.[4] However, this 5-μs burst phase folding lifetime is consistent with estimations that the smallest intrachain loops in an unfolded polypeptide chain will form within 1−3 μs.[17] Since reduction and folding occur almost simultaneously, it is possible that secondary structure formation of this subpopulation of cyt*c* could be faster if the electron could be injected on an even shorter time scale.

Two longer lifetimes, 6 ms and 110 ms, are detected in these TRCD studies, whereas a single 40-ms lifetime is reported by the stopped-flow CD studies in this time region.[20] In this time region the percentage of secondary structure that is formed is similar, with 65% of the native redCyt*c* secondary structure detected in the TRCD studies at 110 ms (our slow phase) and 70% oxCyt*c* native-like structure observed in the stopped-flow CD experiments by 100 ms (their fast phase). During this fast folding phase H-exchange labeling studies indicate that approximately 50% of the helical residues are involved in 30% of the native helical structure.[35] The discrepancy in the content of helix observed between the CD and the NMR results was attributed to other helical structures, such as the 60's and 70's helices or non-native helices, that are not sufficiently stable to provide detectable protection against H-exhange but are measurable by CD methods.

The presence of non-native helices may explain the 180-μs "unfolding" process of the protein that is observed between 16 μs and 1 ms (Figures 3 and 4). Two other explanations may be that native secondary structure folds around a non-native heme ligation or that some folded redCyt*c* undergoes oxidation in this time regime. A "misfolding" implies that unfolding is necessary to ultimately attain the properly folded secondary structure. Thus, the 6-ms process may be a refolding response of the same part of the protein that "unfolds". However, it may not be the only role for the 6-ms process because more protein has folded by 6 ms (30%) than was present before the protein unfolded (25% at 16 μs). This behavior can result if protein folding is inhibited after 16 μs by a misfolding event that prevents completion of burst phase folding. For example, the protein folding may overshoot, forming native or non-native helical structure around a His18-Fe(II)-Met65 (non-native Met) or a bis-His ligation. Before further folding can proceed it might be necessary for the misfolded protein segment to unravel. Clearly, the 6-ms process and the source of the "unfolding" feature cannot be identified without further spectroscopic studies. By examining this time region of redCyt*c* folding in detail we will also have an excellent opportunity to identify misfolded transients and to study their role in protein folding.

In the TRCD experiments, redCyt*c* exhibits 25−30% of its native secondary structure by 4 ms, which is the dead time of the single wavelength stopped-flow CD experiments of oxCyt*c* folding induced by rapid dilution of GdnHCl from 4.7 to 0.7 M.[20] In these stopped-flow CD experiments the burst phase is associated with formation of about 45% of the native secondary structure. The difference in the percentage of secondary structure observed by 4 ms in the TRCD experiments and the stopped-flow experiments is not unusual. At least two of the experimental conditions are different, the concentration of GdnHCl (3.5 M v. 0.7 M) and the cyt*c* species (redCyt*c* versus oxCyt*c*). The optical signals observed during the burst phase in stopped-flow CD studies of oxCyt*c*[36] and RNAse A[37] have been interpreted as a solvent-induced collapse of the polypeptide rather than an intermediate species. This has also been suggested from studies of oxCyt*c* folding using ultrarapid mixing methods coupled with fluorescence[9,38] and resonance Raman[13,14] detection, where the dead times of the experiments are much faster than 1 ms (~45 μs,[39] ~80 μs,[9] and ~100 μs[13,14]). The TRCD studies, which have a time resolution of ~2 μs and which are electron-transfer triggered folding experiments that do not involve any solvent dilutions, detect three distinct intermediates (5 μs, 180 μs, and 6 ms) in the same time regime that is reportedly necessary for the "search−nucleation−collapse" process that precedes protein folding in rapid mixing experiments.[24] These TRCD results suggest that while the protein collapse in the burst phase of oxCytc may result from denaturant dilution there may also be distinct intermediates of the search−nucleation−collapse process which have detectable secondary structure. Studies of oxCytc folding using different folding triggers coupled with various structure sensitive probes which may reveal secondary structure formation within the burst phase would clearly be useful.

Final formation of native secondary structure is preceded by the 110-ms component, which is correlated with Met displacement of His at the heme. This assignment is based predominantly on His dissociation rates observed for oxCytc. According to studies of the denaturant dependence of the refolding rates in oxCytc the dissociation rate of the dominant sixth axial non-native His33 ligand in denatured oxCytc ranges from ~2 to ~8 s^{-1} between 0.5 and 2.75 M GdnHCl.[39] Although comparison of the His dissociation rates in oxCytc with the 110-ms process in redCytc is limited by the denaturant concentrations of the experiments, it should be noted that folded redCytc is more stable in GdnHCl than oxCytc. In addition, the folding rate at a constant free-energy change (0.7 M GdnHCl, 10 °C) for redCytc (115 s^{-1}) is faster than for oxCytc (68 s^{-1}).[2] Thus, the 110-ms process is correlated with displacement of His at the heme. Formation of further secondary structure, facilitated by His displacement, is complete by ~320 ms, at which time the TRCD spectrum is within 90−95% of the equilibrium redCyt*c* spectrum.

The burst and slow folding phases of redCyt*c* are strongly influenced by the identity of the sixth axial heme ligand. The 5-μs folding process most likely involves a Met-binding population, whereas the slower, 110-ms, folding process is defined by a long-lived heme-His ligation that is later displaced by Met. The early TRCD and TROD data suggest the presence of the native His18-Fe(II)-Met heme ligation (Figure 2b) and some secondary structure, which would be consistent with far-UV TRCD and Soret TROD and TRMCD studies of redCyt*c*

(34) Thomas, Y. G.; Chen, E.; Goldbeck, R. A.; Kliger, D. S. Manuscript in preparation.

(35) Roder, H.; Elöve, G. A.; Englander, S. W. *Nature* **1988**, *335*, 700−704.

(36) Sosnick, T. R.; Shtilerman, M. D.; Mayne, L.; Englander, S. W. *Proc. Natl. Acad. Sci. U.S.A.* **1997**, *94*, 8545−8550.

(37) Qi, P. X.; Sosnick, T. R.; Englander, S. W. *Nat. Struct. Biol.* **1998**, *5*, 882−884.

(38) Shastry, M. C. R.; Roder, H. *Nat. Struct. Biol.* **1998**, *5*, 385−392.

(39) Colón, W.; Wakem, P.; Sherman, F.; Roder, H. *Biochemistry* **1997**, *36*, 12535−12541.

folding initiated by COCyt*c* photolysis.[6,7] The intermediate identified at 2 μs in the COCyt*c* studies is characterized by 8% of the native redCyt*c* CD signal and an His18-Fe(II)-Met ligation, whereas ~14% of the redCyt*c* CD signal has formed by 3 μs in these photoinjection studies. Similarly, TRMCD studies of COCyt*c* photolysis[7] shows two conformational subpopulations of cyt*c* molecules that have distinct and parallel folding mechanisms based on the propensity of one to bind Met and the other to bind His. The thermal interconversion between the two protein subpopulations is slow compared to heme rebinding of CO. Such a kinetic heterogeneity is thought to arise from the presence of GdnHCl, which can partially unravel the protein secondary and tertiary structure to form different unfolded states. Although these photoinjection studies have successfully allowed us to monitor protein folding, it cannot directly provide evidence of independent folding pathways. Analysis of the TRMCD data (in progress) on this photoinjection system will help determine if the Met-binding and His-binding populations fold along parallel pathways.

Conclusion

In summary, we show that secondary structure formation in redCyt*c* occurs in two major phases ranging from a few microseconds to hundreds of milliseconds. The TRCD data at times longer than 4 ms correlate well with the secondary structure changes observed in stopped-flow CD experiments.[20] Using electron transfer to trigger the redCyt*c* folding reaction, we are now able to monitor secondary structure dynamics in the burst phase. The reduction step is accompanied by the appearance of secondary structure within 5 μs, and recent TRMCD experimental results[34] provide evidence that the formation of secondary structure can be associated with a Met-ligated subpopulation of protein molecules. The secondary structure stays almost constant until the millisecond time scale, where a small decrease in the magnitude of the CD signal is tentatively associated with a 180-μs "unfolding" phase. Subsequently, an increase in CD signal with a time constant of 6 ms is followed by a 110-ms process that is characterized by formation of the native protein. Whereas the 110-ms component is associated with a subpopulation that is trapped in a bis-His ligation until exchange with Met facilitates folding, the identity of the small 6-ms folding process is still unknown. Details of the transient heme ligations in this cyt*c* system using TROD and TRMCD studies will allow further characterization of the correlation between secondary structure formation and heme ligation or heme misligation states during the folding process.

Acknowledgment. We thank Drs. Robert A. Goldbeck, James W. Lewis, John Winterle, YiRen G. Thomas, Raymond Esquerra for insightful discussions, and Harry B. Gray for support to P.W.S. This work was supported by NIH Grant GM-35158 (D.S.K., E.C.), the Swedish Technical Research Council (P.W.S.), and NSF Grant MCB-9630465 (H.B.G.).

JA983169+